Materials Science-Poland, 29(3), 2012, pp. 189-194
http://www.materialsscience.pwr.wroc.pl/
DOI: 10.2478/s13536-011-0030-8

VERSITA

TiO_2 supported on SiO_2 photocatalysts prepared using ultrasonic-assisted sol-gel method

X.-L. YANG, C.-J. LIU, Y.-Q. LIU, X. LI, Y.-H. XU*

Institute of Biomaterial, College of Science, South China Agricultural University, Guangzhou 510642, Guangdong

TiO_2–SiO_2 (TiO_2 supported on SiO_2) photocatalysts were prepared using an ultrasonic-assisted sol-gel method. These photocatalysts were characterized by X-ray diffraction (XRD), scanning electron microscopy (SEM), Fourier transform infrared spectroscopy (FT-IR) and photoluminescence spectra (PL). Their photocatalytic activities were investigated by the method of methyl orange oxidation. It was found that the photocatalytic activity of TiO_2–SiO_2 was optimal when the molar ratio of hexadecyl trimethyl ammonium bromide to titanium butoxide was 1:10. The average crystallite size of TiO_2–SiO_2 was smaller than that prepared by the stirring method. Furthermore, for pure anatase phase samples, it was shown that the lower the photoluminescence intensity, the higher the photocatalytic activity.

Keywords: *TiO_2–SiO_2, ultrasonic-assisted, X-ray diffraction, photocatalytic property*

1. Introduction

The cavitations produced by ultrasonic treatment can greatly minimize the interaction energy and eliminate the agglomeration of nanoparticles [1]. Numerous studies have demonstrated the importance and advantages of ultrasonication in the improvement of the photocatalytic activities of nano-size TiO_2 particles. The properties of TiO_2, such as the particle size, crystallite size, crystallinity, as well as anatase and rutile phase ratios, can be controlled by the ultrasonic-assisted sol-gel method, and these nano-sized TiO_2 photocatalysts show high photocatalytic activity [2, 3]. In addition, the modified TiO_2 photocatalysts have also been synthesized by ultrasonic-assisted sol-gel method [4, 5]. Huo et al [5] reported that highly active nanocrystalline TiO_2 powders doped with rare earth element – La, were prepared by sol-gel process via ultrasonic irradiation followed by supercritical drying. The ultrasonication and supercritical treatment increased the particle dispersion, crystallinity, the surface oxygen vacancies and/or defects as well as the interaction between the La-dopant and the TiO_2, leading to the higher photocatalytic activity. Nowadays, the ultrasonic technology has become a new method of immobilization [6–8]. For example, Pt, Au and Pd nanoparticles were immobilized onto TiO_2 with the aid of ultrasonic irradiation, and the sonochemically prepared photocatalysts showed higher activities than did the ones prepared by the conventional impregnation method [6]. In this paper, TiO_2–SiO_2 (TiO_2 supported on SiO_2) photocatalysts with surface uniformity and high photocatalytic activity were prepared by ultrasonic-assisted sol-gel method and were characterized using XRD, SEM, FT-IR and PL. The aim of this work is to study the effect of experimental conditions, such as the amount of surfactant, ultrasonic treatment time, and calcination temperature on the physical and chemical properties of TiO_2–SiO_2.

2. Experimental

2.1. Preparation of TiO_2–SiO_2 photocatalysts

A series of TiO_2–SiO_2 photocatalysts was prepared by ultrasonic-assisted sol-gel method. The preparation was carried out as follows: solution A was prepared by adding 45 ml pure alcohol and 3 g diethanolamine to 10 g $Ti(O–Bu)_4$ under stirring, and a molar ratio of $Ti(O–Bu)_4$:EtOH:DEA of 10:234:10 was used. The size of commercial

*E-mail: xuyuehua@scau.edu.cn

SiO_2 (Shanghai Chemical Reagent Co., Ltd.) is in the range of 75–150 μm. 2 g SiO_2, which was heated at 180 °C in a vacuum drying oven for 2 h, was mixed with 50 ml pure alcohol, 0.5 ml distilled water and different amounts of hexadecyl trimethyl ammonium bromide (CTAB) under stirring at constant temperature (25 °C). A molar ratio of CTAB:EtOH:SiO_2:H_2O of 1:260:10:1 was used. When the above adsorption process reached equilibrium after 12 h, the solution A was added dropwise to the adsorption equilibrium system under ultrasonic irradiation in an ultrasonic cleaner (Model KQ-300E, 40 kHz, 300 W, Kun Shan Ultrasonic Instruments Co., Ltd). Subsequently most of the solvent was removed through a rotatory evaporator at 50 °C, and the samples were dried at 70 °C in an oven. So prepared samples were calcined at different temperatures for 1 h and sieved with 75 μm and 150 μm standard sieves, respectively. Hereafter, unless otherwise stated, all TiO_2–SiO_2 photocatalysts were calcined at 500 °C for 1 h.

3. Characterization

The X-ray diffraction (XRD) spectra of the TiO_2–SiO_2 photocatalysts were recorded with a MSAL-XD2 diffractometer (λ = 0.15406 nm) using Cu Kα radiation and standard Bragg-Brentano diffraction geometry. The photoluminescence spectra were recorded by a fluorescence spectrophotometer (RF-530XPC) in order to investigate the relationship between the photocatalytic activity and photoluminescence intensity. The Fourier transform infrared spectroscopy (FI-IR) was carried out with a spectrophotometer (Nicolet 510P). The morphology analysis of TiO_2–SiO_2 was performed using a scanning electron microscope (SEM, FEI-XL30).

3.1. Photocatalytic activity

The schematic diagram of the photocatalytic degradation reactor is shown in Fig. 1. The aqueous suspensions were prepared by adding 0.4 g photocatalyst to 800 ml methyl orange aqueous solution at 20 mg/l. The irradiations were performed with a 125 W high-pressure mercury lamp. The aqueous suspensions were stirred and bubbled with humid oxygen for 30 min prior to the irradiation. The suspension was extracted at 10 minutes intervals. The filtrates were analyzed with a spectrophotometer by measuring their absorbance at 465 nm.

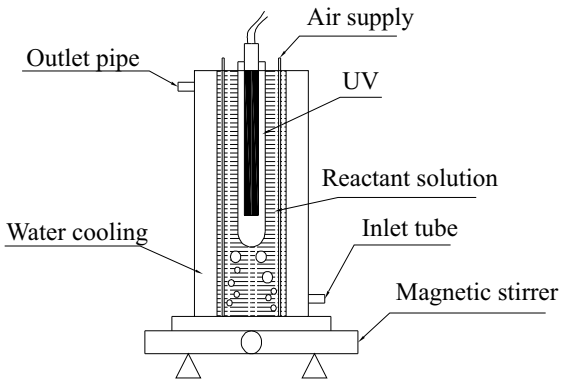

Fig. 1. Schematic diagram of the photocatalytic reactor.

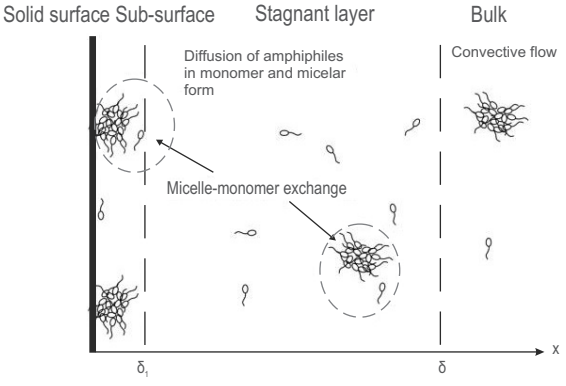

Fig. 2. Schematic picture of adsorption steps of CTAB at SiO_2-water interface.

4. Results and discussion

4.1. Effect of CTAB

Fig. 2 shows the schematic picture of the adsorption process of CTAB on SiO_2-water interface [9], including three process steps, where the first step was CTAB transfer from the bulk solution to a stagnant layer to develop a monomer or micelle due to the convection caused by stirring, the second step was CTAB diffusion from the bulk solution to the subsurface, and the third step was CTAB transportation from the subsurface to the SiO_2 surface and the concomitant adsorption.

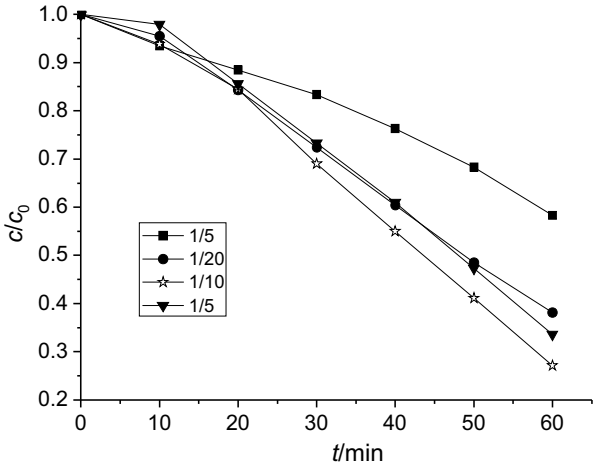

Fig. 3. Effect of different molar ratios of CTAB to TBOT on photocatalytic activities of TiO_2–SiO_2 photocatalysts.

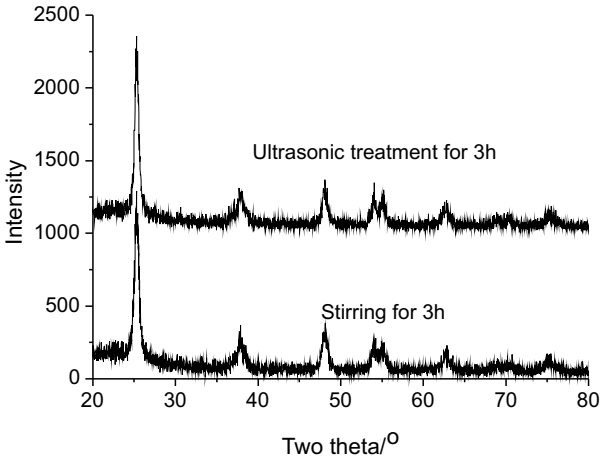

Fig. 4. XRD patterns of TiO_2–SiO_2 prepared by stirring or ultrasonic treatment.

The effect of different molar ratios of CTAB to TBOT on photocatalytic activities of TiO_2–SiO_2 photocatalysts was studied. Fig. 3 shows the plots of c/c_o versus time (t), where c_o and c denote the aqueous phase concentration of methyl orange at $t = 0$ and $t = t$, respectively. The photocatalytic activity of TiO_2–SiO_2 increased with increasing TiO_2 content when the molar ratio of CTAB to TBOT reached 1:10, and then fell. The photocatalytic activity of TiO_2–SiO_2 was the highest when the molar ratio of CTAB to TBOT was 1:10, indicating that the amount of TiO_2 supported on SiO_2 was optimal when the molar ratio of CTAB to TBOT was 1:10.

4.2. Effect of ultrasonic treatment

Fig. 4 shows the XRD patterns of TiO_2–SiO_2 prepared by the stirring method or ultrasonic treatment. The X-ray diffraction peak at 25.4° corresponds to the characteristic peak of the (101) crystal plane of anatase. The average crystallite diameter (D) was calculated by Scherrer's Formula:

$$D = \frac{0.9\lambda}{B\cos\theta} \tag{1}$$

where λ is the X-ray wavelength (0.154178 nm for Cu Kα). B is the peak width at half height, and θ is the Bragg angle. The average crystallite size of TiO_2–SiO_2 prepared by stirring for 3 h was 14.8 nm, and that of TiO_2–SiO_2 prepared by ultrasonic treatment for 3 h was 11.5 nm.

The FT-IR spectra of TiO_2–SiO_2 prepared by stirring or ultrasonic treatment are shown in Fig. 5. The strong bands at 500 cm^{-1} and 1107 cm^{-1} are ascribed to stretching vibration of Ti–O band and Si–O–Si band, respectively, and the weak band at 965 cm^{-1} is assigned to stretching vibration of Ti–O–Si band [10]. The formation of Ti–O–Si band shows that TiO_2 was supported on the surface of SiO_2, and that the SiO_2 interacted with TiO_2. The strong, broad peak at 3433 cm^{-1} and the peak at 1635 cm^{-1} are attributed to the surface-adsorbed water and hydroxyl groups [11]. The peak intensity at 3433 cm^{-1} for TiO_2–SiO_2 prepared by ultrasonic treatment is stronger than that for TiO_2–SiO_2 prepared by stirring, suggesting that more hydroxyl groups were formed on the surface of TiO_2–SiO_2 prepared by the ultrasonic treatment. Hydroxyl groups might trap the holes in the valence band to form surface free radicals ·OH, therefore, leading to generate more ·OH radicals, which are helpful to improve the decomposition rate of methyl orange.

Fig. 6 shows the effect of stirring or ultrasonic treatment on the photocatalytic activities of TiO_2–SiO_2 photocatalysts. As can be seen from Fig. 6, the TiO_2–SiO_2 prepared by ultrasonic treatment showed better photocatalytic activity than that prepared by stirring. Because the high temperature and pressure produced by the ultrasonic cavitations pro-

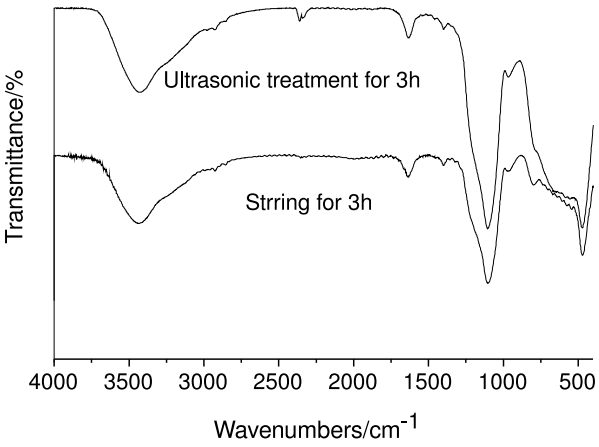

Fig. 5. FT-IR spectra of TiO_2–SiO_2 photocatalysts.

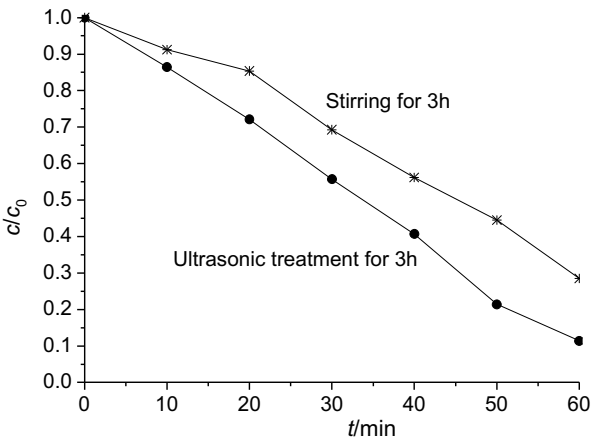

Fig. 6. Photocatalytic activities of TiO_2–SiO_2 photocatalysts prepared by stirring or ultrasonic treatment.

vided the energy for the formation of nuclei, the nuclei formation rate was several orders of magnitude higher than that obtained by stirring method [12]. Moreover, the ultrasonic cavitations produced a large number of tiny air bubbles on the solid surface, which reduced the specific surface free energy of crystallites and inhibited the aggregation and growth of crystallites. At the same time, the high pressure shock waves and microjet produced by the ultrasonic cavitations also broke up the grains [13]. Therefore, the average crystallite size of TiO_2–SiO_2 prepared by ultrasonic treatment was smaller than that of TiO_2–SiO_2 prepared by stirring. The photocatalytic activity of the TiO_2–SiO_2 prepared by ultrasonic treatment was higher than that of TiO_2–SiO_2 prepared by stirring, which was attributed to smaller average crystallite size and higher number of hydroxyl groups.

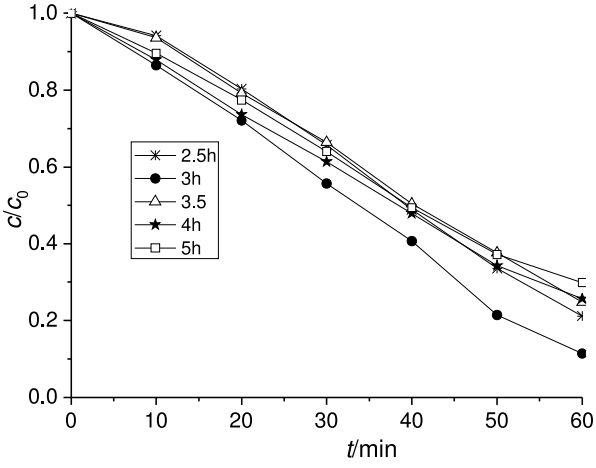

Fig. 7. Effect of different ultrasonic treatment times on photocatalytic activities of TiO_2–SiO_2 photocatalysts.

Fig. 7 shows the effect of different ultrasonic treatment times on the photocatalytic activities of TiO_2–SiO_2 photocatalysts. For the TBOT hydrolysis reaction, the vapor pressure of the reactants was very low, so the chemical effects of the ultrasonic treatment occurred at the boundary between the cavitation bubbles and the aqueous solution [14]. During the ultrasonic treatment, the surfactant CTAB came into contact with the TBOT sol, and the hydrophobic group of CTAB penetrated into the TBOT sol, which was adsorbed onto the surface of SiO_2, in favor of the removal of the organic groups and the formation of Ti–O–Si bond [15]. However, with increasing ultrasonic treatment time, the TBOT sol changed into a suspension, and the amount of TiO_2 supported on SiO_2 reduced. Consequently, the optimum ultrasonic treatment time was 3 h.

4.3. Effect of calcination temperature

Fig. 8 shows the effect of calcination temperature on the photocatalytic activities of TiO_2–SiO_2 photocatalysts. The plots of the photocatalytic activities, ordered from the highest to the lowest, correspond to the temperatures of 500 °C, 600 °C, 450 °C, 700 °C, 800 °C and 900 °C.

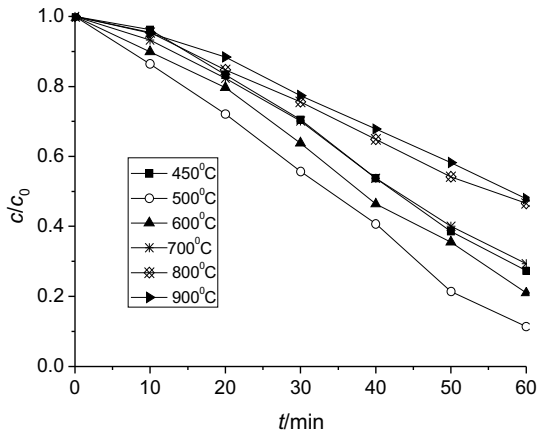

Fig. 8. Photocatalytic activities of TiO_2–SiO_2 photocatalysts calcined at different temperatures.

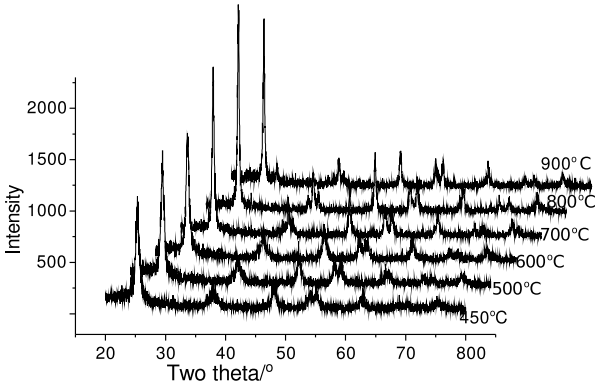

Fig. 9. XRD spectra of TiO_2–SiO_2 photocatalysts calcined at different temperatures.

Fig. 9 shows the XRD spectra of TiO_2–SiO_2 photocatalysts calcined at different temperatures. The crystal phase of all TiO_2–SiO_2 calcined from 450 °C to 700 °C was anatase. After further increasing the calcination temperature up to 800 °C and 900 °C, TiO_2–SiO_2 was composed of mixed anatase-rutile, but even after calcination at 900 °C for 1 h, TiO_2–SiO_2 comprised TiO_2 anatase with a little rutile phase. It was suggested that SiO_2 inhibited the crystal phase transformation of TiO_2, so TiO_2–SiO_2 photocatalysts had good thermal stability at high calcination temperature [16].

Fig. 10 shows the photoluminescence spectra of TiO_2–SiO_2 photocatalysts calcined at different temperatures with the excitation wavelength of 355 nm (λ_{ex} = 355 nm). Photoluminescence is only observed for anatase and rutile phases of TiO_2 whereas amorphous particles show no emission [17]. Apart from the samples calcined at 800 and 900 °C that consisted of both anatase and rutile phase, the photoluminescence peak intensities of TiO_2–SiO_2 photocatalysts, corresponding to pure anatase phase samples, were ordered from high to low at the temperatures of 700, 450, 600, and 500 °C, and the lower the photoluminescence peak intensity, the higher the photocatalytic activity. A large number of defects on the surface of amorphous TiO_2 could become easily the recombination centers of photo-generated electron-hole pairs [18]. However, with increasing calcination temperature, amorphous TiO_2 changed into anatase, which could be beneficial for the photo-generated electron-hole pairs to separate and then migrate to the photocatalyst surface and the generation of hydroxyl radicals [19]. Therefore, the more the electron-hole pairs were separated, the higher photocatalytic activity of TiO_2–SiO_2 was achieved. On the other hand, the photoluminescence spectrum of TiO_2–SiO_2 results from the combination of photo-generated electron-hole pairs [20], so the lower the photoluminescence intensity the higher the photocatalytic activity of TiO_2–SiO_2.

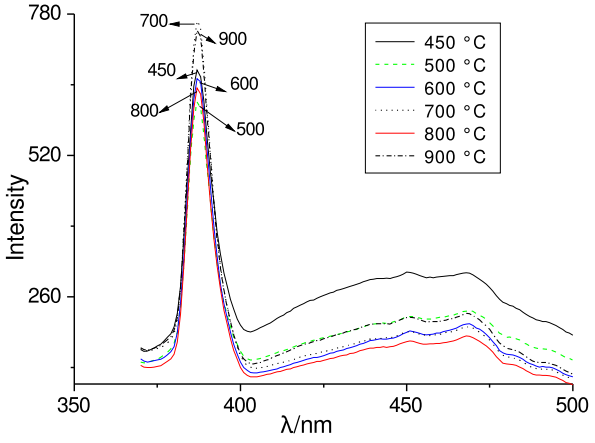

Fig. 10. Photoluminescence spectra of TiO_2–SiO_2 photocatalysts calcined at different temperatures.

Fig. 11 shows the SEM images of SiO_2 and TiO_2–SiO_2. The surface of SiO_2 was smooth, and it could be clearly observed that TiO_2 was immobilized on the surface of TiO_2–SiO_2. The surface of TiO_2–SiO_2 seemed less smooth, meaning that a layer of TiO_2 was obviously present on the surface of SiO_2.

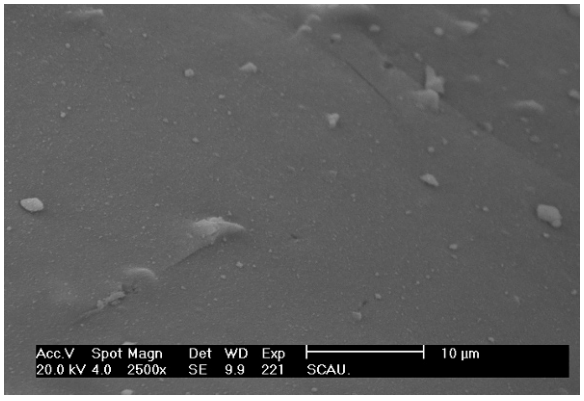

(a)

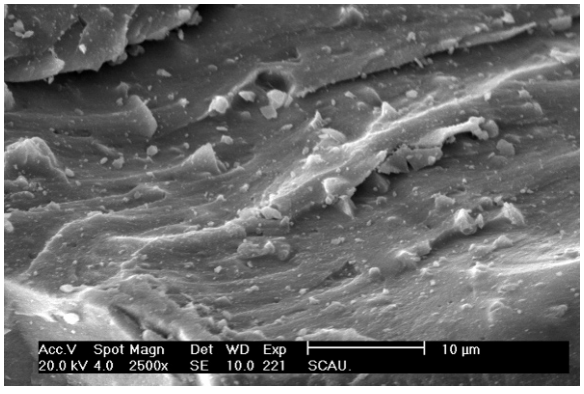

(b)

Fig. 11. SEM images of (a) SiO_2 and (b) TiO_2–SiO_2.

5. Conclusions

TiO_2–SiO_2 photocatalysts with enhanced photocatalytic activities were successfully prepared using ultrasonic-assisted sol-gel method. The average crystallite size of TiO_2–SiO_2 prepared by the ultrasonic treatment was smaller than that of TiO_2–SiO_2 prepared by stirring, and the amount of hydroxyl groups on the surface of TiO_2–SiO_2 prepared using ultrasonic treatment was higher than that on the surface of TiO_2–SiO_2 prepared using stirring method. For the samples with pure anatase phase, it was also found that the lower the photoluminescence intensity, the higher the photocatalytic activity. TiO_2–SiO_2 prepared by ultrasonic treatment for 3 h with a 1:10 molar ratio of CTAB to TBOT followed by annealing at 500 °C for 1 h exhibited the highest photocatalytic activity.

Acknowledgements

The authors would like to thank Guangdong Science & Technology Development Foundation (2007B030103019) and the key Academic Program of the 3rd phase "211 Project" of South China Agricultural University (2009B010100001) for financial supports to this work. We thank Instrumental Analysis & Research Center, South China Agricultural University for assistance with SEM images.

References

[1] YU J.C., YU J., ZHANG L., HO W., *J. Photochem. Photobio. A: Chem.*, 148 (2002), 263.
[2] PRASAD K., PINJARI D.V., PANDIT A.B., MHASKE S.T., *Ultrason. Sonochem.*, 17 (2010), 697.
[3] NEPPOLIAN B., WANG Q., JUNG H., CHOI H., *Ultrason. Sonochem.*, 15 (2008), 649.
[4] RENGARAJ S., YEON J.W., LI X.Z., JUNG Y.J., KIM W.H., *Adv. Nanomater. Process.*, 124–126 (2007), 1745.
[5] HUO Y., J. ZHU, LI J., LI G., LI H., *J. Mol. Catal. A: Chem.*, 278 (2007), 237.
[6] MIZUKOSHI Y., MAKISE Y., SHUTO T., HU J., TOMINAGA A., SHIRONITA S., TANABE S., *Ultrason. Sonochem.*, 14 (2007), 387.
[7] YU Y., YU J.C., YU J.G., KWOK Y.C., CHE Y.K., ZHAO J.C., DING L., GE W.K., WONG P.K., *Appl. Catal. A: Gen.*, 289 (2005), 186.
[8] LIU H., GAO L., *J. Am. Ceram. Soc.*, 89 (2006), 370.
[9] PARIA S., KHILAR K.C., *Adv. Colloid Interfac.*, 110 (2004), 75.
[10] FANG Q., MEIER M., YU J.J., WANG Z.M., ZHANG J.-Y., WU J.X., KENYON A., HOFFMANN P., BOYD I. W., *Mat. Sci. Eng. B*, 105 (2003), 209.
[11] KIM J.-Y., KIM C.-S., CHANG H.-K., KIM T.-O., *Adv. Powder Technol.*, 21 (2010), 141.
[12] WU S., YIN Y., MA Z., QIN Y., QI X., LIANG Z., *Chinese Journal of Molecular Catalysis*, 19 (2005), 167.
[13] GUO W., YANG Z., WANG X., LIN Z., SONG G., *Journal of The Chinese Ceramic Society*, 32 (2004), 1008.
[14] SUSLICK K.S., PRICE G.J., *Annu. Rev. Mater. Sci.*, 29 (1999), 295.
[15] LIU G.Q., JIN Z.G., LIU X.X., WANG T., LIU Z.F., *J. Sol-Gel Sci. Techn.*, 41 (2007), 49.
[16] LI Z., HOU B., XU Y., WU D., SUN Y.H., *J. Colloid Interfac.*, 288 (2005), 149.
[17] MONTICONE S., TUFEU R., KANAEV A.V., *Chem. Phys. Lett.*, 295 (1998), 237.
[18] ISHIBASHI K., FUJISHIMA A., WATANABE T., HASHIMOTO K., *Electroehem. Commun.*, 2 (2000), 207.
[19] HOU Y., LI D., FU X., LIU P., WANG X., *Chinese Journal of Fuzhou University (Natural Sciences Edition)*, 32 (2004), 747.
[20] JUNG K.Y., PARK S.B., ANPO M., *J. Photochem. Photobio. A: Chem.*, 170 (2005), 247.

Received 05.02.2010
Accepted 12.11.2011